Langmuir

Article

pubs.acs.org/Langmuir

Influence of Positional Isomers on the Macroscale and Nanoscale Architectures of Aggregates of Racemic Hydroxyoctadecanoic Acids in Their Molecular Gel, Dispersion, and Solid States

Shibu Abraham,[†] Yaqi Lan,[‡] Ricky S. H. Lam,[§] Douglas A. S. Grahame,[§] Jennifer Jae Hee Kim,[§] Richard G. Weiss,[†] and Michael A. Rogers*[,‡]

[†]Department of Chemistry, Georgetown University, Washington, D.C. 20057-1227, United States

[‡]Department of Food Science, Rutgers University, The State University of New Jersey, New Brunswick, New Jersey 08901, United States

[§]Department of Food and Bioproduct Science, University of Saskatchewan, 51 Campus Drive, Saskatoon, SK, S7N5A8 Canada

ABSTRACT: Inter/intramolecular hydrogen bonding of a series of hydroxystearic acids (HSAs) are investigated. Self-assembly of molecular gels obtained from these fatty acids with isomeric hydroxyl groups is influenced by the position of the secondary hydroxyl group. 2-Hydroxystearic acid (2HSA) does not form a molecular dimer, as indicated by FT-IR, and growth along the secondary axis is inhibited because the secondary hydroxyl group is unable to form intermolecular H-bonds. As well, the XRD long spacing is shorter than the dimer length of hydroxystearic acid. 3-Hydroxystearic acid (3HSA) forms an acyclic dimer, and the hydroxyl groups are unable to hydrogen bond, preventing the crystal structure from growing along the secondary axis. Finally, isomers 6HSA, 8HSA, 10HSA, 12HSA, and 14HSA have similar XRD and FT-IR patterns, suggesting that these molecules all self-assemble in a similar fashion. The monomers form a carboxylic cyclic dimer, and the secondary hydroxyl group promotes growth along the secondary axis.

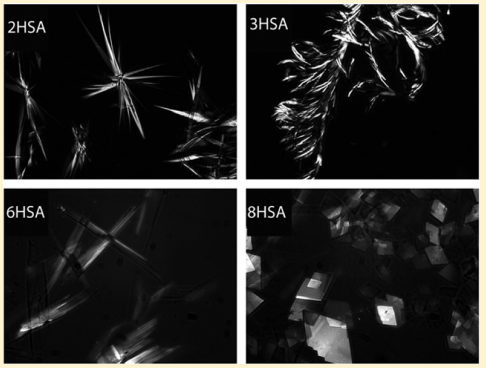

INTRODUCTION

In recent years, molecular gels, composed of low molecular-mass organic gelators (LMOGs), have experienced a surge in interest due to their potential applications and fundamental importance.[1−3] Molecular gels often form a three-dimensional continuous network embedded in a low polarity liquid driven by specific intermolecular interactions to build the primary structures of the fibrillar aggregates.[4] Typically, these physical interactions include H-bonding, electrostatic forces, $\pi-\pi$ stacking, and London dispersion forces.[5] The ability for these molecules to self-assemble into rod-like structures requires a careful balance among opposing parameters including solubility and those that control epitaxial growth into elongated aggregates.[6] On a molecular level, the required characteristics are not well understood. For example, in the same solvent, enantiopure 12-hydroxystearic acid (D-12HSA) forms fibrillar networks, while racemic 12HSA forms platelets.[7−9] Thus, it is extremely important to understand how these physical interactions affect the formation of supramolecular architectures in order to use rational design to discover new classes of low molecular weight organogelators (LMOGs).

As a solution/sol of an LMOG is cooled, the system becomes supersaturated, and eventually the gelator molecules phase-separate microscopically via stochastic nucleation events. Subsequently, in one mode of growth, LMOG molecules diffuse to the surface of the nucleated aggregates and are incorporated into the lattice via highly specific physical interactions that promote one-dimensional growth. Finally, the one-dimensional objects form self-assembled fibrillar networks (SAFiNs).[1] The SAFiNs consist of secondary structures of rods, tubes, ribbons, or even platelets, held together by noncovalent forces,[6] and lead to macroscopic entrapment of the liquid component (and gelation) via capillary forces and interfacial tension within the pores of the network.[1,10] The latter stages of this hierarchical growth can affect profoundly the macroscopic properties of the material, such as its hardness, stability, and oil mobility.[11]

Presented here is an investigation of the molecular characteristics required to promote self-assembly and gelation within a group of positional isomers of racemic hydroxystearic acid. 12HSA, a structurally simple, highly effective LMOG, has been studied extensively for gelation kinetics[12−15] and supramolecular structure formation,[11,16−20] as well as to monitor surface properties,[21] solvent polarity,[5,22] the influence of minor components,[23] and effects of chemical structure.[4,5,7,24−26] We explore how the gelating properties are affected when the position of the hydroxyl group of HSA is moved along the fatty acid backbone. Because the design of new gelators relies heavily

Received: November 9, 2011
Revised: February 12, 2012
Published: February 17, 2012

   dx.doi.org/10.1021/la204412t | *Langmuir* 2012, 28, 4955−4964

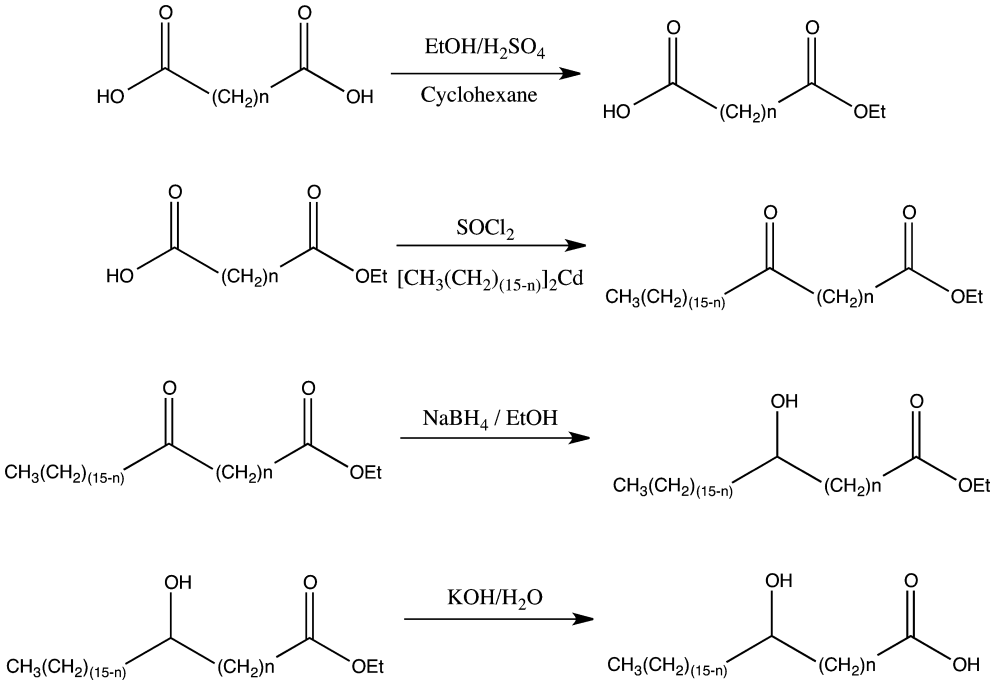

Figure 1. Synthetic pathways to positional isomers of HSA isomers.

on trial and error, and researchers encounter failure more frequently then success, experiments which correlate minor changes in LMOG structure, gelation efficiency, and gel properties can be very useful.[10] For example, modifications of the head group of D-12HSA to amide, amine, and ammonium groups have been shown recently to affect drastically the final properties of the corresponding molecular organo- and hydrogels.[5,27] The aim of this study is to identify factors that influence self-assembly and organogelation of a series of racemic HSA in which the carboxyl head group is unchanged but the position of the hydroxyl group is moved along the alkyl chains.

EXPERIMENTAL SECTION

Materials. Mineral oil (Aldrich), synthetic DL-2-hydroxystearic acid (Matreya, 98%), DL-3-hydroxystearic acid (Matreya, 98%), DL-6-hydroxystearic acid (Materya, 98%), D-12-hydroxysteaic acid (Aldrich, 99%), ethyl acetate (Fischer, HPLC grade), dichloromethane (Fischer, HPLC grade), tetradecanedioic acid (Aldrich, 99%), sebacic acid (Aldrich, 99%), suberic acid (Aldrich, ≥98%), cyclohexane (EMD chemicals, ACS grade, >99%), hexane (Aldrich, HPLC grade), ethanol (The Warner-Graham Company, 190 Proof, 95%), ethanol (Aldrich, anhydrous), $NaHCO_3$ (Aldrich, ReagentPlus, ≥99.5%), KOH (Aldrich, ACS reagent, >85%), and concd hydrochloric acid (EMD chemicals, 36.5−38%) were used as received.

Sample Preparation. A mixture of an HSA in mineral oil was heated to 110 °C and held there for 20 min (to ensure loss of 'crystal history'). The melting temperature was based on differential scanning calorimetry. The solutions/sols were cooled to 30 °C isothermally during the corresponding analysis. Unless stated otherwise, the HSA concentrations were 2.0 wt %.

Instrumentation. NMR spectra in $CDCl_3$ were recorded on a Varian 400 MHz spectrometer with tetramethylsilane (^1H) as the internal standard. Mass spectra were obtained using electron ionization (EI) detector for GC-MS with an Alltech DB-5 (0.25 μm, 30 m × 0.25 mm) column or electron spray ionization (ESI) detector for LC/MS (Varian 500-MS) by direct injection method. Samples were analyzed by gas chromatography using an HP 5980A gas chromatograph with an Alltech DB-5 (0.25 μm, 30 m × 0.25 mm) column and a flame ionization detector. IR spectra were recorded on a Perkin-Elmer Spectrum One FTIR spectrometer interfaced to a computer, using an attenuated total reflection accessory or NaCl plates. Elemental analyses were carried out on a Perkin-Elmer PE2400 microanalyzer, and reported values are averages of three to four measurements.

An AR-G2 rheometer (TA Instruments, New Castle, DE) was used to determine the viscoelastic nature of representative samples. A 10 Pa controlled stress was applied (which was within the linear visoelastic region) while the frequency was swept at 30 °C. Parallel plates (2 cm diameter) were kept at a gap of 1000 um. The critical gelator concentration (CGC) was determined at room temperature for each HSA isomer in mineral oil. The CGCs reported are the lowest concentrations of an HSA for which no flow could be detected after the sample tube was inverted for 30 min.

A Nikon Eclipse E400 light microscope equipped with a Nikon DS-FiL color camera and a long working distance 10Xlens and condenser (Nikon Instruments Inc., Melville, NY) were used to acquire polarized light micrographs. A temperature-controlled stage (LTS120 and PE94 temperature controller (Linkam, Surrey, UK)) was used to control the cooling rates. The image resolution was 2560 by 1920 pixels. Sample preparation consists of taking a drop of the melted sample and spreading it onto a glass microscopy slide.

X-ray diffraction (XRD) was carried out on a Rigaku Multiplex Powder X-ray diffractometer (Rigaku, Japan) with a 1/2 degree divergence slit, 1/2 degree scatter slit, and a 0.3 mm receiving slit, and was set at 40 kV and 44 mA to determine the morphic forms of the HSA networks. Scans were performed from 1° to 35° in 2θ at 0.02θ/min. A Q2000 differential scanning calorimeter (DSC) (TA Instruments) was used to detect the evolution of heat during the exothermic phase transition. Samples (8−10 mg) were hermetically sealed in aluminum pans, and thermograms were collected as the sample was cooled and heated at 2 °C/min. TA analysis software (TA Instruments) integrated the peak and obtained the melting and crystallization enthalpy, and the melting and crystallization temperatures were taken as the peak in the thermograms. Three replicates were performed for this analysis to obtain statistical significance.

Fourier transform infrared (FTIR) spectra were collected using the end station of the mid-IR synchrotron beamline (beamline 01B1-01, Canadian Light Source, Saskatoon, SK). The end station is composed of a Bruker Optics IFS66v/S interferometer coupled to a Hyperion 2000 IR microscope (Bruker Optics, Billerica, MA). Light is focused

dx.doi.org/10.1021/la204412t | Langmuir 2012, 28, 4955−4964

on the sample using a 15× magnification Schwarzschild condenser, collected by a 15× magnification Schwarzschild objective with the aperture set to a spot size of 40 μm × 40 μm, and detected by a liquid nitrogen-cooled narrowband MCT detector utilizing a 100 μm sensing element. A KBr-supported Ge multilayer beam splitter was used to measure spectra in the mid-infrared spectral region. Measurements were performed using OPUS 6.5 software (Bruker Optics). The measured interferograms were an average of 256 scans and were recorded by scanning the moving mirror at 40 kHz (in relation to a reference HeNe laser wavelength of 632.8 nm). The wavelength range collected was 690−7899 cm^{-1} with a spectral resolution of 4 cm^{-1}. Single channel traces were obtained using the fast Fourier transform algorithm, without any zero-filling, after applying a Blackman-Harris 3-Term apodization function. For single spectra, measurements of reference single channel traces were carried out with mineral oil.

Syntheses. *Syntheses of Ethyl Monoesters: Ethyl Hydrogen Suberate, Ethyl Hydrogen Sebacate, and Ethyl Hydrogen Tetradecanedioate.* Ethyl hydrogen suberate, ethyl hydrogen sebacate, and ethyl hydrogen tetradecanedioate were synthesized by Menger's procedure (Figure 1).[21] In a typical reaction, a dicarboxylic acid (7 mmol) was added to a flask containing 360 mL of water, 300 mL of ethanol, and 3 mL of concentrated sulfuric acid. A 200 mL amount of cyclohexane was added to this mixture and stirred vigorously for 24 h, the cyclohexane/ethanol−water mixture was cooled in an ice−water bath and filtered to remove any unreacted diacid, and the cyclohexane layer was separated. The stirring and extraction process was continued (for 3−5 days) until no mono- or diester was found in the cyclohexane layer by TLC analysis (using ethyl acetate as the eluent on silica plate). The cyclohexane layers were combined, and the monoester was separated from diester by extracting the cyclohexane with 1 M aqueous sodium bicarbonate (4 × 150 mL). The aqueous layer was acidified to pH 7 with 1:1 concd hydrochloric acid:water, and monoester was extracted from the aqueous layer with diethyl ether (4 × 100 mL). The combined ether layers were dried over Na_2SO_4, filtered into a round-bottom flask, and concentrated on a rotary evaporator.

Ethyl hydrogen suberate: mp 34−36 °C; yield 64%; ^{1}H NMR ($CDCl_3$, 400 MHz) δ 1.22−1.29 (m, 11H), 1.61−1.63 (m, 4H), 2.24−2.34 (m, 4H), 4.08−4.13 (m, 2H); IR (neat) 2920, 2855, 1735, 1712, 1473, 1430, 1377, 1302, 1227, 1169, 1105, 1047, 1024, 932, 862, 752, 720, 676, 597 cm^{-1}. MS: m/z calculated 230.3; observed 231 (M^+, $C_{12}H_{22}O_4$). Purity ∼99% by GC.

Ethyl hydrogen sebacate: liquid; yield 37%; ^{1}H NMR ($CDCl_3$, 400 MHz) δ 1.23−1.25 (m, 3H), 1.32−1.35 (m, 4H), 1.59−1.64 (m, 3H), 2.15−2.35 (m, 4H), 4.08−4.13 (m, 2H); IR (neat) 2937, 2862, 1709, 1699, 1683, 1447, 1464, 1418, 1374, 1301, 1248, 1186, 1096, 1032, 944, 857 cm^{-1}; MS: m/z calculated 202.3; observed 203 (M^+, $C_{10}H_{18}O_4$). Purity ∼99% by GC.

Ethyl hydrogen tetradecanedioate was also prepared in a similar way, but removal of the diester was not possible by extracting the cyclohexane layer with aqueous sodium bicarbonate (as performed successfully above); the mixture of diester and ketone remained together. This reaction mixture (containing >70% of the desired product) was used for the next step without further purifications.

Syntheses of Keto-Substituted Fatty Acid Esters. The keto-substituted esters of fatty acids were also prepared by Menger's method.[21] In a typical reaction, a Grignard reagent was prepared under a nitrogen atmosphere from magnesium turnings (0.43 g, 0.02 g-atom), 1-bromodecane (3.9 g, 0.02 mol), and 30 mL of anhydrous diethyl ether in a three-neck round-bottom flask at room temperature. All glassware was dried overnight in an oven before reaction, and all reagents were dried before use; *drying is very important to prevent the formation of unwanted side product* (an ester instead of the desired ketone). Anhydrous cadmium chloride (3.3 g, 0.02 mol) was added to the stirred reaction mixture at 0 °C, under a nitrogen atmosphere. Stirring was continued for a few minutes at 0 °C, and then the reaction mixture was refluxed at 40 °C for 1 h. After refluxing, diethyl ether was removed by distillation and 20 mL of dry benzene was added to the flask. Acid chloride was prepared in parallel by refluxing ethyl hydrogen suberate (3.0 g, 0.02 mol) with thionyl chloride (2.6 g, 0.02 mol) for 2 h. The excess thionyl chloride was removed by distillation, and the reaction mixture was purged with nitrogen. Acid chloride, redissolved in dry benzene, was added dropwise to the reaction mixture cooled in an ice bath. After addition, the solution was refluxed for 1 h with stirring. The reaction mixture was then cooled in ice and treated with 10 g of ice and 25 mL of 6 N sulfuric acid. The benzene solution was washed successively with 50 mL of water, 5% aqueous sodium bicarbonate (25 mL), water (40 mL), and 10% aqueous sodium chloride (25 mL). The benzene solution was dried over anhydrous sodium sulfate, and benzene was distilled off under vacuum in a rotary evaporator. The compound was then purified by column chromatography using 10:90 (v:v) ethyl acetate:hexane to obtain 3.4 g of ethyl 8-oxooctadecanoate as a solid in 52% yield.

Ethyl 8-oxooctadecanoate: mp 37.6−38.2 °C (lit. mp 37 °C[1]); ^{1}H NMR ($CDCl_3$, 400 MHz) δ 0.88−0.89 (m, 3H), 1.25−1.63 (m, 27H), 2.28−2.40 (m, 6H), 4.09−4.15 (m, 2H); IR (neat) 2954, 2927, 2849, 1734, 1704, 1462, 1379, 1323, 1276, 1239, 1221, 1239, 1176, 1130, 1108, 1040, 990, 969, 867, 800, 764, 750, 728, 720, 684 cm^{-1}. MS: m/z calculated 326.5; observed 327 (M^+, $C_{20}H_{38}O_3$). Purity ∼99% by GC.

Ethyl 10-oxooctadecanoate: liquid; ^{1}H NMR ($CDCl_3$, 400 MHz) δ 0.88−0.89 (t, 3H), 1.24−1.63 (m, 27H), 2.26−2.40 (m, 6H), 4.09−4.15 (m, 2H); IR (neat) 2932, 2851, 1733, 1706, 1410, 1374, 1300, 1230, 1187, 1035, 932, 754, 725, 680 cm^{-1}. MS: m/z calculated 326.5; observed 327 (M^+, $C_{20}H_{38}O_3$). Purity ∼99% by GC.

Ethyl 14-oxooctadecanoate was also prepared in a similar way (i.e., via the Grignard synthesis) and passed through a silica gel column using 1:19 ethyl acetate:hexane, but all fractions contained diester as an impurity. The total ethyl 14-oxooctadecanoate from all fractions, 5.4 g (1.7 mmol), was hydrolyzed to 14-oxooctadecanoic acid by refluxing with 2.5 N KOH (18 mL) in ethanol (20 mL) for 4.5 h followed by acidification to pH 7 using 1:1 concd hydrochloric acid:water. The precipitated solid was extracted with dichloromethane (4 × 25 mL) and purified using a silica gel column with 1:9 ethyl acetate:hexane as the eluent to get 3.4 g of 14-oxooctadecanoic acid in 69% yield. 14-Oxooctadecanoic acid: mp 80.8−82.5 °C. ^{1}H NMR ($CDCl_3$, 400 MHz) δ 0.89−0.92 (m, 3H), 1.26−1.65 (m, 24H), 2.33−2.41 (m, 6H); IR (neat) 2915, 2849, 1698, 1463, 1430, 1382, 1348, 1329, 1305, 1261, 1233, 1211, 1187, 1187, 1128, 1054, 938, 909, 766, 728, 720, 684, 624, 603 cm^{-1}. MS-ESI: m/z calculated 298 + 23; observed 321 (M + Na, $C_{18}H_{34}O_3$).

Syntheses of Hydroxy Fatty Acid Esters. The carbonyl group was reduced to hydroxyl using $NaBH_4$/ethanol as described below. In a typical reaction, ethyl 10-oxooctadecanoate (1.8 g, 5.4 mmol) was added to 40 mL of anhydrous ethanol with stirring at room temperature under an air atmosphere; the mixture was warmed slightly to dissolve the ketone. Sodium borohydride (0.21 g, 5.4 mmol) was added to this solution, and the reaction mixture was stirred at room temperature for 1.5 h. Excess sodium borohydride was destroyed by adding glacial acetic acid slowly, using a pipet, until reaching pH < 5. Ethanol and acetic acid were evaporated using a rotary evaporator; the remaining yellowish-white residue was dried under house vacuum for an additional 12 h. The resulting mixture was purified by column chromatography using 1:19 ethyl acetate:hexane as eluent.

Ethyl 10-hydroxyoctadecanoate: yield (71%), mp 44.7−45.7 °C, ^{1}H NMR ($CDCl_3$, 400 MHz) δ 0.86−0.90 (t, 3H, J = 6.8 Hz), 1.24−1.63 (m, 31H), 2.27−2.30 (t, 2H, J = 7.6 Hz), 3.58 (m, 1H), 4.10−4.15 (q, 2H, J = 7 Hz); IR (neat) 3393, 2922, 2852, 1737, 1421, 1467, 1395, 1331, 1254, 1178, 1131, 1100, 1028, 890, 861, 794, 751, 722, 655 cm^{-1}. MS: m/z calculated 328.5; observed 351 (M + Na, $C_{20}H_{38}O_3$). Purity ∼99% by GC.

Ethyl 8-hydroxyoctadecanoate: yield (63%), mp 45.5−46.5 °C, ^{1}H NMR ($CDCl_3$, 400 MHz) δ 0.86−0.90 (t, 3H, J = 6.6 Hz), 1.24−1.63 (m, 31H), 2.27−2.31 (t, 2H, J = 7.6 Hz), 3.58 (m, 1H), 4.10−4.15 (q, 2H, J = 7.2 Hz); IR (neat) 3441, 2917, 2849, 1734, 1466, 1380, 1315, 1254, 1259, 1220, 1236, 1198, 1182, 1113, 1067, 1048, 1032, 996, 919, 887, 856, 840, 792, 764, 750, 724 cm^{-1}. MS: m/z calculated 328.5; observed 351 (M + Na, $C_{20}H_{38}O_3$). Purity ∼99% by GC.

dx.doi.org/10.1021/la204412t | *Langmuir* 2012, 28, 4955−4964

Syntheses of Racemic Hydroxy Fatty Acids. Esters of the hydroxyl-substituted fatty acids were hydrolyzed to obtain the corresponding fatty acids.[21] In a typical procedure, ethyl 8-hydroxyoctadecanoate (1.4 g, 4.3 mmol) was refluxed with 95% ethanol (10 mL) and 9 mL of 2.5 N aqueous KOH for 4.5 h. After the reaction, ethanol was evaporated, and the reaction mixture was diluted with 50 mL of water. The resulting solution was acidified to pH 7 with 1:1 concd hydrochloric acid:water. The precipitated solid was filtered and dried at 60 °C for 24 h. It was recrystallized from acetone to obtain 1.1 g (84%) of 8-hydroxyoctadecanoic acid.

8-Hydroxyoctadecanoic acid (8HSA): mp 80.6−82.4 °C (lit. mp 78.5−79 °C[31]); ^{1}H NMR ($CDCl_3$, 400 MHz) δ 0.86−0.90 (t, 3H, J = 6.8 Hz), 1.26−1.67 (m, 28H), 2.33−2.37 (t, 2H, J = 7.4 Hz), 3.58 (m, 1H); IR (neat) 3374, 2916, 2849, 1734, 1693, 1464, 1433, 1314, 1297, 1280, 1263, 1240, 1228, 1204, 1194, 1131, 1115, 1103, 1047, 1022, 996, 898, 857, 839, 720 cm $^{-1}$. MS-ESI: m/z calculated 300.5; observed 323 (M + Na, $C_{18}H_{36}O_3$). Elemental analysis for $C_{18}H_{36}O_3$; C 71.95, H 12.08 (calculated); C 71.92, H 12.53 (observed).

10-Hydroxyoctadecanoic acid (10HSA): yield (72%), mp 78.1−79.3 °C; ^{1}H NMR ($CDCl_3$, 400 MHz) δ 0.86−0.90 (t, 3H, J = 6.8 Hz), 1.28−1.65 (m, 28H), 2.32−2.36 (t, 2H, J = 7.4 Hz), 3.58−3.6 (m, 1H); IR (neat) 3389, 2919, 2849, 1714, 1690, 1465, 1433, 1337, 1315, 1295, 1281, 1260, 1223, 1192, 1132, 1116, 1101, 1033, 997, 891, 842, 795 cm $^{-1}$; MS-ESI: m/z calculated 300.5; observed 323 (M + Na, $C_{18}H_{36}O_3$); Elemental analysis for $C_{18}H_{36}O_3$;C 71.95, H 12.08 (calculated); C 72.11, H 12.52 (observed).

Synthesis of Racemic 12-Hydroxystearic Acid (12HSA). D-12HSA (3.0 g, 10 mmol) was added to a stirred solution of $Na_2Cr_2O_7$ (2.1 g, 7.0 mmol) in 3−5 mL of DMSO. Concd H_2SO_4 (2.0 g, 2.5 equiv) was added dropwise with stirring, maintaining the temperature below 80 °C. The mixture was heated and stirred at 70 °C for 2 h and stirred for an additional 12 h at ambient temperature. The reaction mixture was poured into ice-cold water, and the solid that precipitated was filtered. The solid was chromatographed using a silica gel column and 1:9 ethyl acetate:hexane as eluent. After recrystallization from acetone, 1.0 g (33%) of 12-oxooctadecanoic acid was obtained as an off-white solid, mp 78.7−81.4 °C. ^{1}H NMR ($CDCl_3$, 400 MHz) δ 0.86−0.90 (m, 3H), 1.27−1.65 (m, 24H), 2.33−2.40 (m, 6H); purity ∼99% by GC.

The 12-oxooctadecanoic acid was reduced to 12HSA by $NaBH_4$ in ethanol.[21] In a typical reaction, 12-oxooctadecanoic acid (1 g, 3 mmol) was added to 25 mL of absolute ethanol with stirring at room temperature. The solvent was warmed slightly to dissolve the compound. Sodium borohydride (0.1 g, 3 mmol) was then added, and the mixture was stirred at room temperature for 1.5 h. Excess sodium borohydride was destroyed by neutralizing with glacial acetic acid. The ethanol and acetic acid were removed under vacuum, and the yellowish-white residue was dried under vacuum for an additional 12 h. It was washed with water (4 × 30 mL), dried, and recrystallized from acetone to yield 0.90 g (96%) of DL-12HSA, mp 74.9−76.9 °C (lit. mp 76.2 °C).[25] ^{1}H NMR ($CDCl_3$, 400 MHz) δ 0.87−0.90 (t, 3H, J = 6.6 Hz), 1.28−1.65 (m, 28H), 2.17−2.36 (t, 2H, J = 7.4 Hz), 3.58−3.60 (m, 1H); IR (neat) 3327, 2915, 2849, 1706, 1464, 1436, 1410, 1328, 1314, 1295, 1277, 1263, 1241, 1222, 1189, 1133, 1116, 1081, 1026, 1000, 920, 898, 861, 837, 794, 728, 721, 684, 631, 619, 605 cm^{-1}. Analytical data for $C_{18}H_{36}O_3$: C 71.95, H 12.08 (calculated); C 71.54, H 12.62 (observed).

Synthesis of Racemic 14-Hydroxyoctadecanoic Acid (14HSA). 14-Oxooctadecanoic acid was reduced to its hydroxyl derivative using $NaBH_4$/ethanol. In a typical reaction, 14-oxooctadecanoic acid (1.4 g, 4.3 mmol) was added to 25 mL of ethanol with stirring at room temperature (solution was slightly warmed to dissolve the compound). Sodium borohydride (0.12 g, 4.3 mmol) was then added to this solution, and the reaction mixture was stirred at room temperature for 1.5 h. Excess sodium borohydride was destroyed by neutralizing with glacial acetic acid. The ethanol and acetic acid were evaporated on a rotary evaporator; the remaining residue was dried under vacuum for an additional 12 h. It was then extracted with water (4 × 30 mL), dried, and recrystallized from acetone. The product contained a small amount of the starting material, and repeated crystallizations did not remove it. The reaction was carried out at higher temperatures and at refluxing conditions, but a small amount of starting material remained unreacted. As noted below, this material melted over a range of 5.1 °C. It was purified by column chromatography using silica gel after converting the acid to an ester (see below). 14-Hydroxyoctadecanoic acid: mp 70.5−75.6 °C. ^{1}H NMR ($CDCl_3$, 400 MHz) δ 0.89−0.92 (m, 3H), 1.27−1.65 (m, 33H), 2.33−2.37 (m, 3H), 0.359 (s, 1H); IR (neat) 2915, 2848, 1698, 1463, 1430, 1382, 1305, 1283, 1262, 1233, 1211, 1187, 1128, 1054, 938, 909, 766, 728, 720, 684, 624, 603 cm^{-1}. MS-ESI: m/z calculated 300 + 23; observed 323 (M + Na, $C_{18}H_{36}O_3$).

Synthesis of Methyl 14-Hydroxyoctadecanoate. Impure 14-hydroxyoctadecanoic acid from above was esterified using methanol/H_2SO_4 mixtures. In a typical reaction, 14-hydroxyoctadecanoic acid (485 mg, 1.6 mmol) dissolved in 20 mL of methanol and 1 mL of concentrated H_2SO_4 was refluxed for 12 h. The reaction mixture was then cooled, and excess methanol was evaporated under reduced pressure using a rotary evaporator. The residual solid was then extracted using dichloromethane (4 × 20 mL), and the combined extracts were washed with water and dried over anhydrous Na_2SO_4. The dichloromethane was evaporated on a rotary evaporator, and the product was further purified by silica gel column chromatography using 1:19 ethyl acetate:hexane as the eluent to get 386 mg (76% yield; ∼99% pure by GC) of methyl 14-hydroxyoctadecanoate, mp 52.6−54.6 °C. ^{1}H NMR ($CDCl_3$, 400 MHz) δ 0.89−0.93 (t, 3H, J = 7 Hz), 1.26−1.43 (m, 28H), 2.28−2.32 (t, 2H, J = 7.8 Hz), 3.59 (s, 1H), 3.67 (s, 3H); IR (neat) 3477, 2916, 2849, 1739, 1464, 1435, 1383, 1359, 1314, 1295, 1275, 1254, 1238, 1222, 1198, 1174, 1134, 1116, 1062, 1046, 1018, 993, 973, 952, 885, 864, 793, 759, 728, 702, 603 cm^{-1}.

Methyl 14-hydroxyoctadecanoate (300 mg, 0.95 mmol) was refluxed with 95% ethanol (10 mL) and 9 mL of 2.5 N aqueous KOH for 4.5 h. Ethanol was evaporated, and the reaction mixture was diluted with 50 mL of water. The resulting solution was acidified with a solution of concd hydrochloric acid and water in a 1:1 ratio. The precipitated solid was filtered and dried at 60 °C for 24 h. The white solid was recrystallized from acetone to obtain 276 mg (90%) of 14-hydroxyoctadecanoic acid, mp 75.8−77.7 °C. ^{1}H NMR ($CDCl_3$, 400 MHz) δ 0.89−0.93 (t, 3H, J = 7 Hz), 1.26−1.67 (m, 28H), 2.33−2.36 (t, 2H, J = 7.4 Hz); IR (neat) 3494, 3387, 2916, 2849, 1738, 1464, 1435, 1383, 1359, 1314, 1296, 1275, 1222, 1198, 1175, 1134, 1117, 1061, 1046, 1018, 993, 974, 884, 864, 793, 759, 728, 702, 624, 604 cm^{-1}. MS-ESI: m/z calculated 300 + 23; observed 323 (M + Na, $C_{18}H_{36}O_3$).

RESULTS AND DISCUSSION

Viscous solutions instead of gels were formed when sols of up to 2 wt % 2HSA or 3HSA in mineral oil were cooled from 110 °C to 30 °C isothermally (i.e., the sol was placed on the Peltier plate at the preset temperature). Mineral oil samples at the 2.0 wt % 6HSA, 8HSA, 10HSA, 12HSA, and 14HSA could be inverted in a glass vial and did not exhibit flow. Rheological measurements confirmed that the mineral oil samples of 2 wt % samples of 6HSA, 8HSA, 10HSA, 12HSA, and 14HSA are true gels (Figure 2). Their G' values are virtually independent of frequency over a very broad range. Further, G' is greater than G''. However, 2HSA and 3HSA were not and exhibited a G'/G'' crossover. At this time, the strength of the gel samples is known only qualitatively. Although none of the HSA were capable of gelating mineral oil at concentrations <1 wt %, which would make them 'supergelators', they were able to form gels at relatively low concentrations. The CGCs were found to be ∼1.7 wt % for 12HSA and 14HSA and ∼1.9 wt % for 6HSA, 8HSA, and 10HSA.

Early work on 12HSA organogels indicated the presence of a SAFiN whose nature is dependent on the ability of the carboxylic acid head groups to dimerize and the secondary hydroxyl groups on the fatty acid backbone to form hydrogen-bonding arrays.[5,8,29] All of the HSA/mineral oil dispersions, whether viscous liquids or gels, were opaque. The opacity or

dx.doi.org/10.1021/la204412t | *Langmuir* 2012, 28, 4955−4964

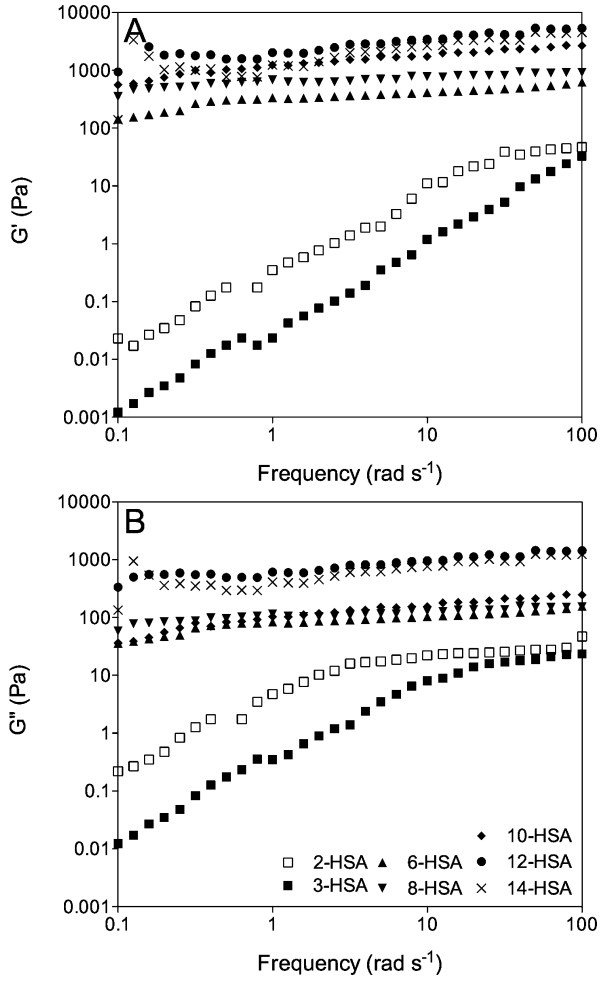

Figure 2. Frequency sweeps for the positional isomers of gels and dispersion of 2 wt % HSA isomers in mineral oil at 30 °C.

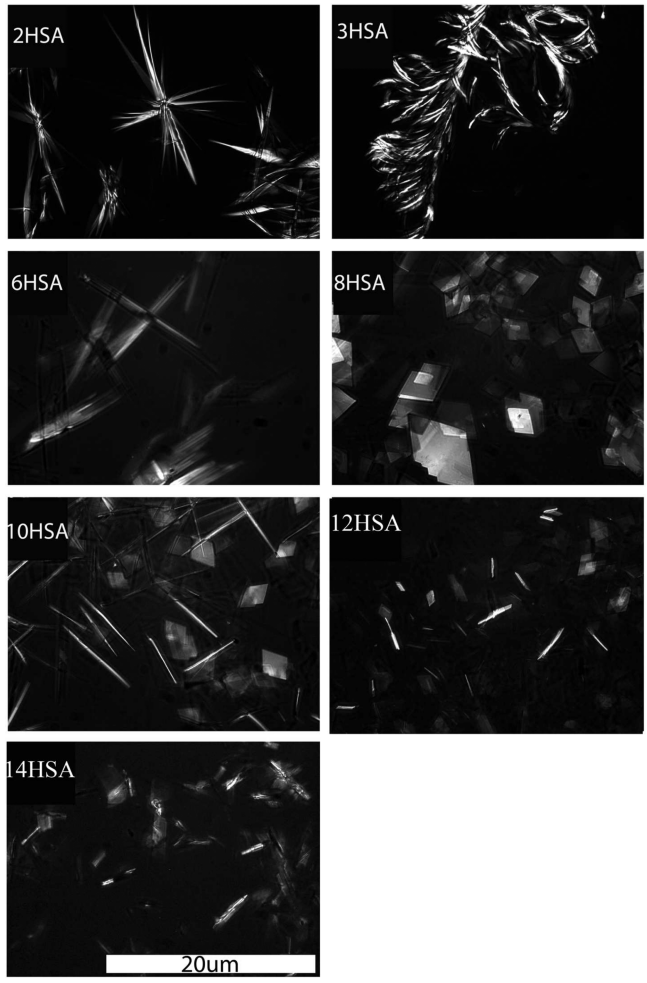

Figure 3. Polarized light micrographs of positional isomers of 2 wt % gels and dispersions of HSA in mineral oil at 30 °C. The space bar applies to all panels.

transparency of an organogel is directly related to the cross-sectional thickness of the crystalline aggregates, the number of junction zones capable of diffracting light, and the number of crystalline aggregates within the self-assembled network.[30,31] The smaller the constituents of a SAFiN network, the more transparent the gel.

Polarized light micrographs (Figure 3) provided information about the shapes of the crystalline objects constituting the supramolecular network within the gels. The appearances of the dispersions with 2HSA and 3HSA differed dramatically from those of the gels with 6HSA, 8HSA, 10HSA, 12HSA, and 14HSA (Figure 3). The crystal morphology of 2HSA in mineral oil indicated that few nuclei were present and that crystal growth occurred as fibers growing in a radial fashion from nucleating centers (Figure 3). However, it is obvious that the domains of the separate crystals do not interpenetrate, which inhibits the formation of a continuous crystal network and an organogel. Similarly, the appearance of the 3HSA micrograph suggests that even fewer nucleation points occur and that the crystal growth results in highly branched fibers. Hydroxystearic acids with the hydroxyl group at or beyond position 6 on the fatty acid backbone form orthorhombic crystal platelets and fibers. In these systems, many more crystalline centers are present, indicating more nucleating sites formed during the initial stages of SAFiN growth and less subsequent crystal growth. The large number of small platelets and fibers interpenetrate, forming a three-dimensional network capable of entrapping the liquid component. The presence of platelets for these systems was expected because they are racemic mixtures, and previous work has shown that DL-12HSA results in platelets whereas D- or L-12HSA provides fibers.[7,25] None of the crystal morphologies resemble enantiopure 12HSA and the sense of helical twist due to the racemic nature of these compounds.

With drastic differences in the microstructure, the nanostructure was probed to correlate with the crystal morphology. X-ray diffraction (XRD) was used to measure the wide- and short-angle spacings of the neat solid and the organogels and dispersion (Figure 4, Table 1). The molecular packing of each HSA in its neat solid and dispersion/gel phases differ in at least one aspect; the materials from solvent crystallizations (see Experimental Section) and from cooling the mineral oil sols have different morphologies. However, all of the HSA in both the neat solid and dispersion/gel phases are stacked in lamellar structures with thicknesses about twice the extended molecular length (46 Å) according to analyses of the diffractograms.[5] In the gels of 6HSA to 14HSA, the secondary hydroxyl groups form a hydrogen bonding array along the axis of the fibers in the gels, vide infra.[20,29] The wide-angle diffractions yield spacings consistent with at least two morphic forms, including orthorhombic (3.8 and 4.2 Å) and triclinic (4.6 Å).[32]

dx.doi.org/10.1021/la204412t | Langmuir 2012, 28, 4955−4964

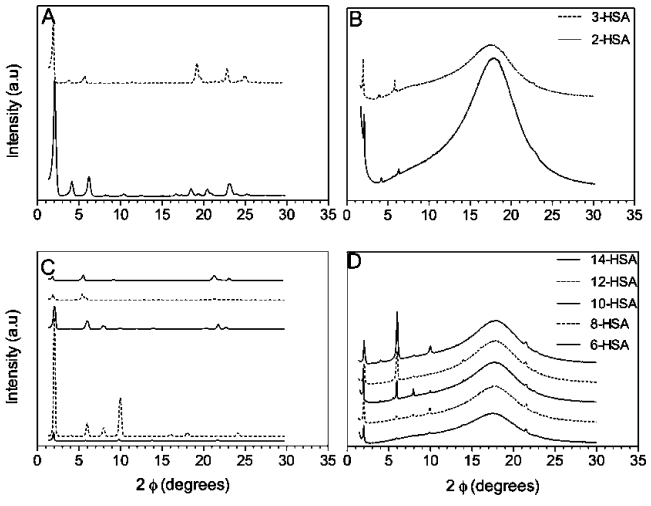

Figure 4. Vertically offset XRD patterns at 30 °C for neat (A, C) and 2 wt % HSA in mineral oil (B, D). The line designations in B and D apply to A and C, respectively.

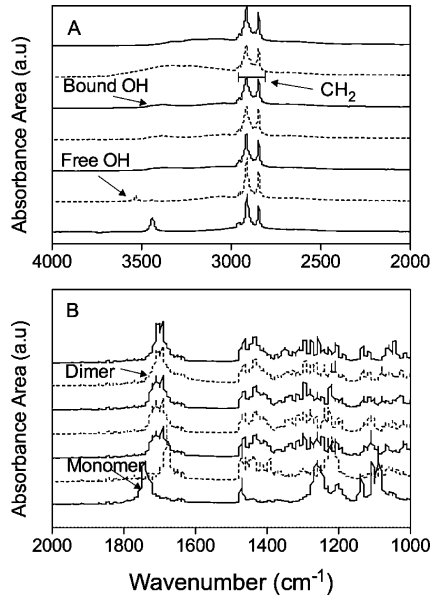

Figure 5. Vertically offset FT-IR spectra of the hydroxyl region (A) and carboxylic acid region (B) positional isomers of neat HSA isomers. The spectra start with 2HSA at the bottom, increasing to 14HSA at the top.

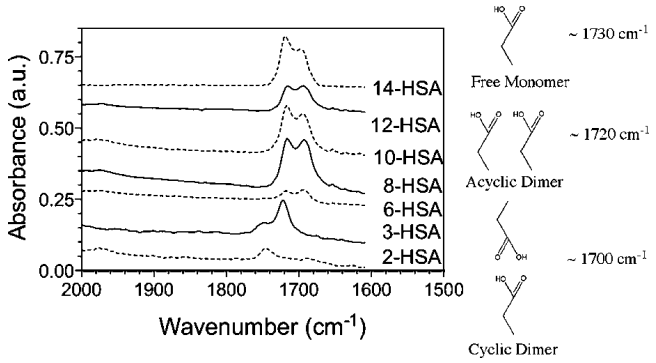

Figure 6. Vertically offset FT-IR spectra of positional isomers of gels/dispersions of 2 wt % HSA isomers in mineral oil.

The short-angle spacings, in the gels and dispersions are ~43−45 Å with corresponding higher order reflections in the expected progression for lamellae. However, both the neat solid and mineral oil dispersion of 2HSA have a slightly shorter spacing, ~41−42 Å. Furthermore, the dispersions of 2HSA and 3HSA lack a detectable wide-angle spacing while the gels of 6HSA, 8HSA, 10HSA, 12HSA, and 14HSA all have a single wide-angle peak corresponding to ~4.1 Å, consistent with hexagonal packing of the fatty acid chains within a layer.[32] It appears that the transition from the platelet-like crystals (i.e., HSA with hydroxyls at carbon 6 and beyond) to the fiber-like crystals (i.e., 2HSA and 3HSA) (Figure 3) corresponds to the absence of a wide-angle spacing (Table 1).

With obvious differences in the crystal packing, FT-IR was used to probe the chemical environments of the carboxylic acid head groups in the solid state (Figure 5) and in their organogels and dispersions (Figure 6). This technique was previously used to observe the changes from a cyclic dimer to acyclic dimer in 12HSA mixtures of varying enantiomeric excess (from optically pure to racemic).[7] Carboxylic acid groups may have three distinct chemical environments depending on the interactions

Table 1. Distances (Å) and Reflection Attributions Calculated from Bragg's Law from X-ray Diffractograms in the Mineral Oil Gels, Dispersions, and Neat Powders of HSA Positional Isomers

		small-angle diffractions						
isomer	state	001	002	003	004	005	006	wide-angle diffractions
2HSA	neat	42.43	21.22	14.15	10.74	8.54	7.07	4.78; 4.60; 4.43; 3.84; 3.52
	dispersion	41.16	20.93	13.98				no reflection
3HSA	neat	46.95	23.48	15.65		9.32	7.70	4.62; 3.89; 3.56
	dispersion	44.15	23.00	15.13		8.90		no reflection
6HSA	neat	44.61	22.62	15.22	11.36	9.03	7.48	4.35; 4.09; 3.92; 3.76
	gel	44.17		14.92		8.90	6.35	4.12
8HSA	neat	43.26	22.18	14.77	11.04	8.87		4.93; 3.69
	gel	44.11		14.91	11.15	8.91		4.12
10HSA	neat	42.85	21.96	14.82	11.11	8.89	6.34	4.36; 4.08; 3.91; 3.74
	gel	42.88		14.72	11.07	8.90	6.33	4.14
12HSA	neat	47.46	24.25	16.29	11.27	9.69	8.08	6.02; 4.37; 4.14; 3.87
	gel	45.46		14.82	11.10	8.87	6.33	4.13
14HSA	neat	48.49	24.12	16.06	12.00	9.61	8.01	4.76; 4.17; 3.85, 3.74
	gel	43.67	21.96	14.67	10.99	8.84		4.13

dx.doi.org/10.1021/la204412t | Langmuir 2012, 28, 4955−4964

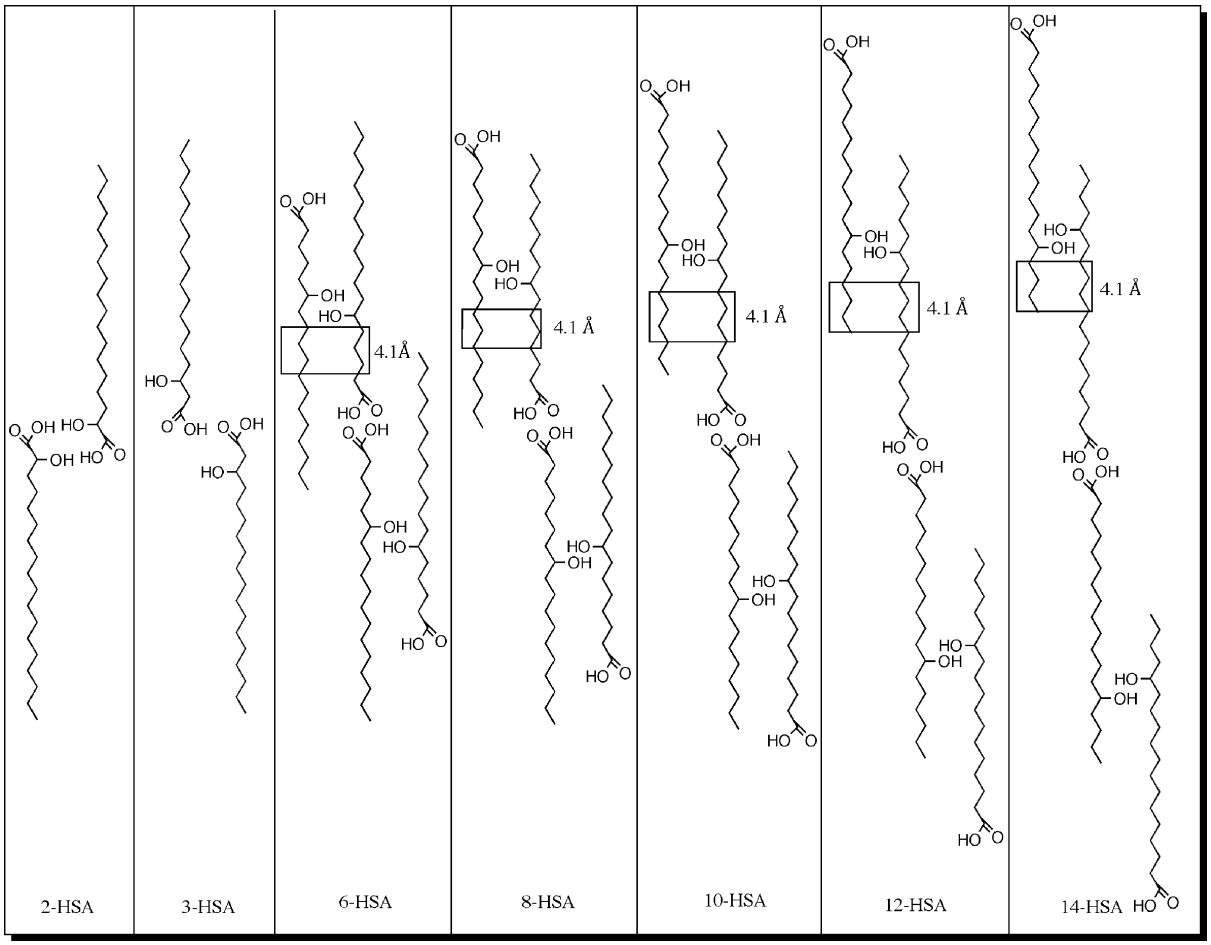

Figure 7. Proposed packing arrangements of HSA isomers in the SAFiNs of their gels/dispersions in mineral oil. Distances shown are based on XRD measurements.

with other carboxylic acids. They may exist as a free monomer (~1730 cm^{-1}), an intermolecular acyclic dimer (~1720 cm^{-1}), or an intermolecular cyclic dimer (~1700 cm^{-1}).[7,33] The 2HSA mineral oil dispersion has an IR spectrum significantly different than that of the other hydroxystearic acid dispersions and organogels (Figure 6). The IR spectra suggest that 2HSA remains as a 'monomer' in the crystal structure and that 3HSA has spectral features of both a free monomer (1730 cm^{-1}) and acyclic dimer (1720 cm^{-1}). In the solid state, 2HSA remains as the free monomer, and 3HSA in the solid state has a single peak that may correspond to the acyclic dimer (Figure 5B). 6HSA through 14HSA have similar distributions of both acyclic dimers and cyclic dimers in their solid state (Figure 5B) and organogels (Figure 6) due to the presence of two peaks at 1720 and 1700 cm^{-1}. In the solid state, 2HSA and 3HSA have free OH stretches while 6–14HSA have bound hydroxyl groups (Figure 5A)

From both the XRD and FT-IR data, it appears that modifying the position of the secondary hydroxyl group has significant effects on the packing arrangements of the hydroxyl and carboxyl groups within the gel/dispersion phases. The lack of dimers in the mineral oil dispersion of 2HSA (Figure 6), as well as the lack of wide-angle diffractions characteristic of highly organized chains within a layer (Table 1), indicates that when the secondary hydroxyl group is very close to the carboxylic acid head group, extensive hydrogen bonding of the secondary hydroxyl groups along the second axis is absent. Hence, we postulate that the molecular packing of 2HSA promotes (or exists because of) carboxyl–hydroxyl interactions and is a primary reason why its lamellar spacing is shorter than those of the other HSA isomers (Figure 7) and why the carboxylic acid groups are not in dimeric arrangements. 3HSA dispersion forms an acyclic dimer (Figure 6), and no X-ray diffraction corresponding to a short spacing is observed. The long spacing is equal to the dimer length (Figure 7). Similar to 2-HSA dispersions, the secondary hydroxyl group is in proximity to the carboxylic group and does not promote growth along the secondary axis.

As mentioned, the fibers and platelets of gels of 6HSA, 8HSA, 10HSA, 12HSA, and 14HSA exhibit an XRD diffraction peak corresponding to approximately twice the length of an extended HSA molecule (Table 1). FT-IR spectra of these samples, as well as those of the neat powders (Figure 5), indicate that the molecular pairs constituting a lamellar thickness are arranged in acyclic and cyclic orientations of their carboxyl groups (Figure 6) and the XRD diffractograms show a peak corresponding to ~4.1 Å in 2θ. This suggests that the hydroxyl group must be located at a distance from the carboxylic acid group to promote crystal growth along the secondary axis (Figure 6).

Crystallization of 2 wt % HSAs in mineral oil is an exothermic transition (Figure 8A). The amount of heat per gram of gelator released during self-assembly of the HSA in mineral oil depends on the position of the hydroxyl group on

dx.doi.org/10.1021/la204412t | *Langmuir* 2012, 28, 4955–4964

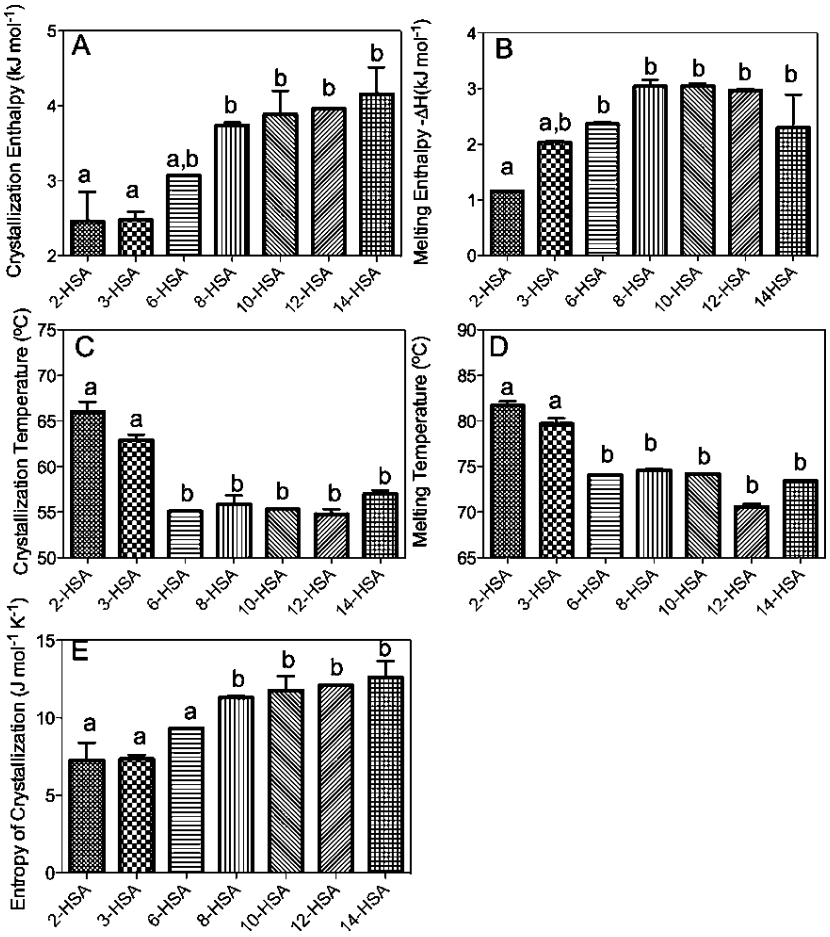

Figure 8. Crystallization enthalpy (A), melting enthalpy (B), temperature (C), temperature (D), and entropy (E) of isomers of 2 wt % HSA in their gels/dispersions in mineral oil. Statistical analysis was performed using one-way ANOVAs and a Tukey's postanalysis test ($p > 0.05$) and the labels a and b indicate statistical differences between the HSAs.

the alkyl chain. When the hydroxyl group is at position 2 or 3, significantly less heat is evolved compared to the isomers with hydroxyls at carbon 8, 10, 12, or 14 (Figure 8A). Similarly, the endothermic melting requires significantly less energy for 2HSA and 3HSA (Figure 8B.). The heat released during crystallization and absorbed during melting is a function of the energy of the new physical interactions which accompany the self-assembly. In the case of hydroxylated fatty acids, this is primarily a function of hydrogen bonding of the carboxylic acid and secondary hydroxyl groups and London dispersion forces. The lower energy associated with the transition from sol to gel of 2HSA and 3HSA is consistent with the lack of their effective carboxyl dimerization and the inability of their secondary hydroxyl groups to interact, as mentioned above. The broadness of the melting curves makes an accurate measurement of the areas under them (and thus the enthalpies of melting) difficult and subject to significant error. The crystallization enthalpies are much more accurate because the cooling exotherms are much narrower, and it is easier to establish a baseline for the peaks. As we have selected the heating curve baselines, the melting enthalpies are lower than those of the crystallizations.

Crystallization temperatures (Figure 8C) and melting temperatures (Figure 8D) of 2HSA and 3HSA dispersions are at temperatures higher than those of gels of the other positional isomers. The crystallization and melting temperatures were determined at the points of maximum heat flow. The crystallization temperature (K) and crystallization enthalpy (ΔH) have been used to calculate a change in the entropy ($\Delta S = \Delta H/T$) (Figure 8E) during the sol-to-gel/dispersion transitions. A similar trend to the ΔH was observed in the ΔS changes: the entropies of 2HSA and 3HSA are significantly lower than those of the 8−14HSA isomers. This observed trend was expected because the polar carboxylic acid head group and secondary hydroxyl group are very close, at one end of the molecule, while the hydrophobic aliphatic chain constitutes the other end of the molecule. This arrangement allows the polar head groups to be more effectively shielded from the low polarity solvent, i.e., mineral oil in the sol. Hence, for 2HSA and 3HSA, HSA−HSA interactions are stronger than those of the 6−14HSAs which have stronger interactions between the low polarity solvent and the polar entities of the molecule.

■ CONCLUSIONS

The supramolecular aggregation forms and nanostructures of SAFiNs in hydroxystearic acid gels in mineral oil, a low polarity liquid, are affected acutely by the position of the hydroxyl group position on the LMOG. When the hydroxyl group is at position 2, the HSA molecules do not dimerize effectively and growth along the secondary axis of the aggregate network is inhibited. Interaction between the head groups of 2HSA results in a Bragg distance for the longest dimension of the dimers that is significantly shorter than the sum of the extended lengths of

dx.doi.org/10.1021/la204412t | Langmuir 2012, 28, 4955−4964

two molecules; they are partially interdigitated. The XRD data also indicate that 3HSA forms acyclic dimers in which the hydroxyl groups are unable organize into an effective H-bonding network along a secondary axis. Finally, based on the similarity of the XRD and FT-IR patterns of the SAFiNs of 6HSA, 8HSA, 10HSA, 12HSA, and 14HSA, their nanostructures and overall packing arrangements appear to be similar. These HSA are able to form effectively both carboxylic cyclic dimers and H-bonding networks via their hydroxyl groups.

These results demonstrate that a systematic analysis of the molecular packing in aggregates of structurally simple molecules, such as the HSA, at the nanometer and even subnanometer distance scales can lead to meaningful correlations with their aggregates at the micrometer and even larger distance scales. In addition, the results reported here provide a basis for addressing a very important and largely unresolved question: How do such aggregates form in real time? This and other basic aspects of SAFiN formation by HSAs will be addressed in the future.

AUTHOR INFORMATION

Corresponding Author

*E-mail: rogers@AESOP.Rutgers.edu.

Notes

The authors declare no competing financial interest.

ACKNOWLEDGMENTS

S.A. and R.G.W. thank the U.S. National Science Foundation for support of this research.

REFERENCES

(1) Terech, P.; Weiss, R. G. Low Molecular Mass Gelators of Organic Liquids and the Properties of Their Gels. *Chem. Rev.* **1997**, 3133−3159.

(2) Abdallah, A. J.; Weiss, R. G. Organogels and low molecular mass organic gelators. *Adv. Mater. (Weinheim, Ger.)* **2000**, *12*, 1237−1247.

(3) Weiss, R. G.; Terech, P., Introduction. In *Molecular Gels: Materials with Self-Assebled Fibrillar Networks*; Weiss, R. G.; Terech, P., Eds.; Springer: Dordrecht, The Netherlands, 2006; pp 1−13.

(4) Terech, P.; Rodriguez, V.; Barnes, J. D.; McKenna, G. B. Organogels and Areogels of Racemic and Chiral 12-Hydroxyoctadecanoic Acid. *Langmuir* **1994**, *10* (10), 3406−3418.

(5) Mallia, V. A.; George, M.; Blair, D. L.; Weiss, R. G. Robust Organogels from Nitrogen-Containing Derivatives of (*R*)-12-Hydroxystearic Acid as Gelators: Comparisons with Gels from Stearic Acid Derivatives. *Langmuir* **2009**, *25* (15), 8615−8625.

(6) Suzuki, M.; Nakajima, Y.; Yumoto, M.; Kimura, M.; Shirai, H.; Hanabusa, K. Effects of hydrogen bonding and van der Waals interactions on organogelation using designed low-molecular-weight gelators and gel formation at room temperature. *Langmuir* **2003**, *19* (21), 8622−8624.

(7) Grahame, D. A. S.; Olauson, C.; Lam, R. S. H.; Pedersen, T.; Borondics, F.; Abraham, S.; Weiss, R. G.; Rogers, M. A. Influence of Chirality on the Modes of Self-Assembly of 12-Hydroxystearic Acid in Molecular Gels of Mineral Oil. *Soft Matter* **2011**, *7*, 7359−7365.

(8) Tachibana, T.; Kambara, H. Sense of twist in fibrous aggregates from 12-hydroxystearic acid and its alkali metal soaps. *J. Colloid Interface Sci.* **1968**, *28* (1), 173−178.

(9) Tachibana, T.; Mori, T.; Hori, K. Chiral Mesophases of 12-Hydroxyoctadecanoic Acid in Jelly and in the Solid State. I. A New Type of Lyotropic Mesophase in Jelly with Organic Solvents. *Bull. Chem. Soc.* **1980**, *53*, 1714−1719.

(10) Li, J. L.; Lui, X. Y. Architecture of Supramolecular Soft Functional Materials: From Understanding to Micro-/Nanoscale Engineering. *Adv. Funct. Mater.* **2010**, *20*, 3196−3216.

(11) Wang, R. Y.; Liu, X. Y.; Narayanan, J.; Xiong, J. X.; Li, J. L. Architecture of Fiber Network: From Understanding to Engineering of Molecular Gels. *J. Phys. Chem. B* **2006**, *10*, 25797−25802.

(12) Terech, P. Kinetics of Aggregation in a Steroid Derivative/Cyclohexane Gelifying System. *J. Colloid Interface Sci.* **1985**, *107* (1), 244−255.

(13) Rogers, M. A.; Marangoni, A. G. Non-Isothermal Nucleation and Crystallization of 12-Hydroxystearic Acid in Vegetable Oils. *Cryst. Growth Des.* **2008**, *8* (12), 4596−4601.

(14) Lam, R.; Quaroni, L.; Pederson, T.; Rogers, M. A. A molecular insight into the nature of crystallographic mismatches in self-assembled fibrillar networks under non-isothermal crystallization conditions. *Soft Matter* **2010**, *6* (2), 404−408.

(15) Lam, R. S. H.; Rogers, M. A. Experimental Validation of the Modified Avrami Model for Non-Isothermal Crystallization Conditions. *CrystEngComm* **2010**, *13*, 866−875.

(16) Li, J. L.; Liu, X. Y.; Wang, R. Y.; Xiong, J. Y. Arichitecture of a Biocompatible Supramolecular Material by Supersaturation-Driven Fabrication of its Network. *J. Phys. Chem. B* **2005**, *109*, 24231−24235.

(17) Li, J. L.; Wang, R. Y.; Liu, X. Y.; Pan, H. H. Nanoengineering of a Biocompatible Organogel by Thermal Processing. *J. Phys. Chem. B* **2009**, *113* (15), 5011−5015.

(18) Rogers, M. A.; Wright, A. J.; Marangoni, A. G. Engineering the oil binding capacity and crystallinity of self-assembled fibrillar networks of 12-hydroxystearic acid in edible oils. *Soft Matter* **2008**, *4* (7), 1483−1490.

(19) Rogers, M. A.; Wright, A. J.; Marangoni, A. G. Corrigendum to "Nanostructuring fiber morphology and solvent inclusions in 12-hydroxystearic acid/canola oil organogels" [Current Opinion in Colloid & Interface Science 14(1) (2009) 33−42]. *Curr. Opin. Colloid Interface Sci.* **2009**, *14*, (3), 223.

(20) Rogers, M. A.; Wright, A. J.; Marangoni, A. G. Nanostructuring fiber morphology and solvent inclusions in 12-hydroxystearic acid/canola oil organogels. *Curr. Opin. Colloid Interface Sci.* **2009**, *14* (1), 33−42.

(21) Menger, F. M.; Richardson, S. D.; Wood, M. G.; Sherrod, M. J. Chain-Substituted Lipids in Monomolecular Films. Effect of Polar Substituents on Molecular Packing. *Langmuir* **1989**, *5*, 833−838.

(22) Rogers, M. A.; Marangoni, A. G. Solvent-Modulated Nucleation and Crystallization Kinetics of 12-Hydroxystearic Acid: A Non-isothermal Approach. *Langmuir* **2009**, *25* (15), 8556−8566.

(23) Fameau, A. L.; Houinsou-Houssou, B.; Novales, B.; Navailles, L.; Nallet, F.; Douliez, J. P. 12-Hydroxystearic acid lipid tubes under various experimental conditions. *J. Colloid Interface Sci.* **2010**, *341* (1), 38−47.

(24) Huang, X.; Weiss, R. G. Molecular organogels of the sodium salt of (R)-12-hydroxystearic acid and their templated syntheses of inorganic oxides. *Tetrahedron* **2007**, *63* (31), 7375−7385.

(25) Sakurai, T.; Masuda, Y.; Sato, H.; Yamagishi, A.; Kawaji, H.; Atake, T.; Hori, K. A Comparative Study on Chiral and Racemic 12-Hydroxyoctadecanoic Acids in the Solutions and Aggregation States: Does the Racemic Form Really Form a Gel? *Bull. Chem. Soc.* **2010**, *83* (2), 145−149.

(26) Wright, A. J.; Marangoni, A. G. Time, temperature, and concentration dependence of ricinelaidic acid-canola oil organogelation. *J. Am. Oil Chem. Soc.* **2007**, *84* (1), 3−9.

(27) Mallia, V. A.; Terech, P.; Weiss, R. G. Correlations of Properties and Structures at Different Length Scales of Hydro- and Organogels Based on *N*-Alkyl-(*R*)-12-Hydroxyoctadecylammonium Chlorides. *J. Phys. Chem. B* **2011**, *115*, 12401−12414.

(28) Menger, F. M.; Richardson, S. D.; Wood, M. G.; Sherrod, M. J. *Langmuir* **1989**, *5*, 833.

(29) Kuwahara, T.; Nagase, H.; Endo, T.; Ueda, H.; Nakagaki, M. Crystal structure of DL-12-hydroxystearic acid. *Chem. Lett.* **1996**, *25*, 435−436.

(30) Terech, P.; Pasquier, D.; Bordas, V.; Rossat, C. Rheological properties and structural correlations in molecular gels. *Langmuir* **2000**, *16*, 4485−4494.

(31) Tamura, T.; Ichikawa, M. Effect of lecithin on organogel formation of 12-hydroxystearic acid. *J. Am. Oil Chem. Soc.* **1997**, *74* (5), 491−495.
(32) Marangoni, A. G. Crystallography. In *Fat Crystal Networks*; Marangoni, A. G., Ed.; Marcel Dekker: New York, 2005; pp 1−20.
(33) Lin-Vien, D.; Colthup, N. B.; Fateley, W. G.; Grasselli, J. G. *The Handbook of Infrared and Raman Characteristic Frequencies of Organic Molecules*; Academic Press: London, UK, 1991.